Depolarization-induced suppression of excitation in murine autaptic hippocampal neurones

Alex Straiker and Ken Mackie

Department of Anaesthesiology, University of Washington, Seattle, WA 98195, USA

Depolarization-induced suppression of excitation and inhibition (DSE and DSI) appear to be important forms of short-term retrograde neuronal plasticity involving endocannabinoids (eCB) and the activation of presynaptic cannabinoid CB1 receptors. We report here that CB1-dependent DSE can be elicited from autaptic cultures of excitatory mouse hippocampal neurones. DSE in autaptic cultures is both more robust and elicited with a more physiologically relevant stimulus than has been thus far reported for conventional hippocampal cultures. An additional requirement for autaptic DSE is filled internal calcium stores. Pharmacological experiments favour a role for 2-arachidonyl glycerol (2-AG) rather than arachidonyl ethanolamide (AEA) or noladin ether as the relevant endocannabinoid to elicit DSE. In particular, the latter two compounds fail to reversibly inhibit EPSCs, a quality inconsistent with the role of bona fide eCB mediating DSE. Δ^9-Tetrahydrocannabinol (Δ^9-THC) fails to inhibit EPSCs, yet readily occludes both DSE and EPSC inhibition by a synthetic CB1 agonist, WIN 55212-2. With long-term exposure (∼18 h), Δ^9-THC also desensitizes CB1 receptors. Lastly, a functional endocannabinoid transporter is necessary for the expression of DSE.

(Received 2 June 2005; accepted after revision 20 September 2005; first published online 22 September 2005)
Corresponding author A. Straiker: Department of Anaesthesiology, University of Washington, Seattle, WA 98195, USA. Email: straiker@u.washington.edu

Endocannabinoids are thought to serve as retrograde messengers, allowing neurones to regulate, via feedback inhibition, their upstream neuronal inputs. This suppression of upstream presynaptic release of GABA or glutamate (along with coreleased neurotransmitters) is termed depolarization-induced suppression of inhibition (DSI) or excitation (DSE), respectively. DSI was first reported in the early 1990s (Llano *et al.* 1991; Vincent *et al.* 1992), coincidently not long after the cloning of the first cannabinoid receptor (Matsuda *et al.* 1990), but a decade would pass before the link between the two was discerned (Kreitzer & Regehr, 2001*a*,*b*; Ohno-Shosaku *et al.* 2001; Wilson & Nicoll, 2001). Subsequently, it has become clear that the endogenous cannabinoid signalling system mediates both DSI and its excitatory cousin, DSE (Kreitzer & Regehr, 2001*b*; Ohno-Shosaku *et al.* 2002). Endocannabinoids have now been found to serve an inhibitory role in many regions of the brain (e.g. Kreitzer & Regehr, 2001*a*; Melis *et al.* 2004; Trettel *et al.* 2004), lending support to the hypothesis that mediation of feedback inhibition is one of their principal functions.

Numerous questions remain unanswered regarding DSE, which was first described 10 years after DSI. Among these questions are the identity of the endocannabinoid, the relationship between Δ^9-tetrahydrocannabinol (Δ^9-THC) and DSE, and the role of the endocannabinoid membrane transporter. Research into DSE has been hindered by the lack of accessible culture models, since in conventional hippocampal culture DSE is weak and follows only in response to a harsh stimulus (Ohno-Shosaku *et al.* 2002). DSE in autaptic neurones might offer advantages; specifically, a well-characterized isolated glutamatergic preparation allowing simultaneous pre- and postsynaptic measurements with a single electrode. Furthermore, development of a murine autaptic DSE preparation makes possible the study of genetically altered mice, such as those engineered to lack the CB1 receptor or components of the eCB signalling cascade. Thus we undertook to ascertain whether murine cultured autaptic hippocampal neurones might indeed express DSE, and thereby serve to address some unanswered questions regarding DSE.

Methods

Culture preparation

All procedures used in this study were approved by the Animal Care Committee of the University of Washington and conform to the Guidelines of the National Institutes

 DOI: 10.1113/jphysiol.2005.091918

of Health on the Care and Use of Animals. Mouse (CD1 or, in the case of FAAH–/– animals, C57/Bl6) hippocampal neurones isolated from the CA1–CA3 region were cultured on microislands as previously described (Furshpan *et al.* 1976; Bekkers & Stevens, 1991). Neurones were obtained from animals (age postnatal day 0–2, killed via rapid decapitation without anaesthesia) and plated onto a feeder layer of hippocampal astrocytes that had been laid down previously (Levison & McCarthy, 1991). Cultures were grown in high-glucose (20 mM) type medium containing 10% horse serum, without mitotic inhibitors, and used for recordings after 8 days in culture and for no more than 3 h after removal from culture medium. Drugs were tested on cells from at least two different preparations.

Electrophysiology

When a single neurone is grown on a small island of permissive substrate, it forms synapses, or 'autapses', onto itself. All experiments were performed on isolated autaptic neurones.

Whole cell voltage-clamp recordings from autaptic neurones were carried out at room temperature using an Axopatch 200A amplifier (Axon Instruments, Burlingame, CA, USA). The extracellular solution contained (mM): 119 NaCl, 5 KCl, 2.5 $CaCl_2$, 1.5 $MgCl_2$, 30 glucose, 20 Hepes, 0.1 picrotoxin (to block inhibitory $GABA_A$-mediated currents) and 3 μM bovine serum albumin (as a carrier for the lipophilic endocannabinoids). Continuous flow of solution through the bath chamber (1–2 ml min^{-1}) ensured rapid drug application and clearance. Drugs were typically prepared as stock solutions, then diluted into extracellular solution at their final concentration and used on the same day. Drugs dissolved in DMSO were used at a final DMSO concentration of $< 0.1\%$. As a rule, positive results were coupled on the same day with negative controls. Conversely, negative results for a given drug (e.g. WIN 55212-2 in CB1–/– neurones) were coupled on the same day with positive controls for that drug in control cells.

Recording pipettes of 1.5–5 MΩ resistance were filled with (mM): 121.5 potassium gluconate, 17.5 KCl, 9 NaCl, 1 $MgCl_2$, 10 Hepes, 0.2 EGTA, 2 MgATP and 0.5 LiGTP. Access resistance was monitored, and only cells with stable access resistance were included for data analysis.

Stimulus protocols

Two major sets of stimulus protocols were used in these experiments, one to elicit DSE, the other for conventional EPSC studies such as dose–response studies.

DSE stimulus protocol. After establishing a 10–20 s 0.5 Hz baseline, DSE was evoked by depolarizing to 0 mV for 1–10 s, followed by resumption of a 0.5 Hz stimulus protocol for from 10 to > 80 s, as necessary. A 0.5 Hz baseline stimulus frequency was used for the sake of temporal resolution. We did not observe a potentiation of EPSCs as a result of this DSE stimulus.

Conventional stimulus protocol. The membrane potential was held at –70 mV and EPSCs were evoked every 20 s by triggering an unclamped action current with a 1.0 ms depolarizing step. The resultant evoked waveform consisted of a brief stimulus artifact, a large downward spike that represented inward sodium currents, followed by the slower EPSC. The size of the recorded EPSCs was calculated by integrating the evoked current to yield a charge value (in pC). Calculating the charge value in this manner yields an indirect measure of the amount of neurotransmitter released while minimizing the effects of cable distortion on currents generated far from the site of the recording electrode (the soma). Data were acquired at a sampling rate of 5 kHz.

Effects of DSE on paired-pulse responses were studied by paired trials in which two pulses (60 ms interval) were applied immediately before and 4 s after a DSE-evoking depolarizing stimulus. The amplitude ratios of the pre-DSE pairs and the post-DSE pairs were averaged and compared via paired Student's *t* test.

Recent work (e.g. Kelley & Thayer, 2004*a*) has demonstrated a distressing promiscuity on the part of several cannabinoid-related pharmacological agents. In several cases we obtained negative data in the absence of positive controls (e.g. cyclo-oxygenase type 2 (COX-2) inhibition has no effect on DSE). In each instance the concentrations of the drugs were taken from the high end of published results; however, negative results must as a rule be interpreted with care.

Materials

Endocannabinoid transporter inhibitor (UCM-707), 2-arachidonyl glycerol (2-AG), arachidonyl ethanolamide (AEA) and FAAH inhibitor (URB-597) were purchased from Cayman Chemical Co. (Ann Arbor, MI, USA). All remaining drugs were purchased from Tocris Cookson (Ellisville, MO, USA) or Sigma-Aldrich (St Louis, MO, USA). CB1–/– and FAAH–/– mice were generously provided by Drs Catherine Ledent (UFR de Medicine & Pharmacie, Roven, France; Reibaud *et al.* 1999) and Ben Cravatt (Scripps Research Institute, San Diego, CA, USA; Cravatt *et al.* 2001), respectively.

Results

Glutamatergic autaptic cultured hippocampal neurones exhibit DSE

We found that depolarization of glutamatergic autaptic hippocampal neurones for 1–10 s reduced EPSC size for ~1 min (EPSC size expressed as charge in pC; Fig. 1*A*).

Average inhibition was comparable to that obtained with the CB1 agonist, WIN 55212-2 (0.54 ± 0.05 of control, $n = 13$; WIN 55212-2 (100 nM): 0.46 ± 0.04 of control, $n = 17$; Fig. 1*C*). Minimal inhibition occurred in neurones cultured from mice lacking the CB1 receptor (0.95 ± 0.02 of control, $n = 7$; Fig. 1*B* and *C*). Furthermore, pre- and co-incubation with the CB1 antagonist, SR 141716A (100 nM), blocked the depolarization-induced inhibition, indicating a CB1 dependence (0.87 ± 0.03 of control, $n = 6$; Fig. 1*C*). The depolarization additionally increased the paired-pulse ratio, consistent with a presynaptic site of action (Fig. 1*D*). We will hereafter refer to this inhibition as DSE.

Autaptic excitatory hippocampal neurones express functional CB1 receptors (Sullivan, 1999), but purely autaptic DSE was somewhat unexpected. Nonetheless, autaptic DSE compares favourably with DSE in conventionally cultured neurones both in terms of maximal inhibition and duration of the stimulus required to elicit DSE. Maximal inhibition averaged 46%, considerably greater than the 20% inhibition reported for conventionally cultured hippocampal neurones, and often approached the 90% seen for DSI in culture (Ohno-Shosaku *et al.* 2002). The difference is not due to the use of integral (*versus* peak) measurements of EPSCs (e.g. 0.50 ± 0.06 of control (integral) *versus* 0.54 ± 0.06 of control (peak), $n = 5$). In addition to being robust, DSE remained stable, declining only slightly over the course of a 10 min recording (same cell: 0.57 ± 0.06 *versus* 0.62 ± 0.03 (10 min later), $n = 5$).

What stimulus is required to induce autaptic DSE?

Previously it has been reported that 10 s depolarizations were necessary to elicit DSE (Ohno-Shosaku *et al.* 2002). We observed that as little as 1 s of depolarization was often sufficient to elicit robust DSE (Fig. 2*A* and *B*). We found that by progressively extending depolarization times we reached a saturating or maximal inhibition, defined as that inhibition where a longer subsequent depolarization resulted not in greater inhibition but rather in slower recovery (often several minutes in duration). For example, the neurone shown in Fig. 2*C* exhibits nearly maximal inhibition with 1 s depolarization and a half-life ($t_{1/2}$) decay time of 11 s. Increasing the duration of depolarization only modestly increases the inhibition, but substantially increases the $t_{1/2}$ value (3 s depolarization: $t_{1/2} = 24$ s; 10 s depolarization: $t_{1/2} = 57$ s). The period of depolarization required to reach saturation varied from cell to cell and typically ranged from 1 to 10 s.

In principle, a high-frequency (100 Hz) stimulus might mimic depolarization-induced DSE with a more physiologically relevant stimulus. However, since an autaptic neurone is clamped both pre- and postsynaptically and depolarization of the latter is thought to be required for DSE (Diana & Marty, 2004), a high-frequency stimulus might not be expected to elicit DSE in a cell otherwise held at a potential of –70 mV. To test this we stimulated neurones with a 2.5 s series of 1 ms depolarizations at 100 Hz. As predicted, this stimulus protocol did not induce robust DSE (Fig. 2*D*, $n = 6$), though the brief inhibition observed was blocked by the CB1 antagonist, SR 141716A (100 nM, data not shown).

Determinants of maximal DSE inhibition

Some neurones exhibited very little DSE, whereas in others the maximal inhibition by DSE approached the 90% seen in conventionally cultured hippocampal DSI. What

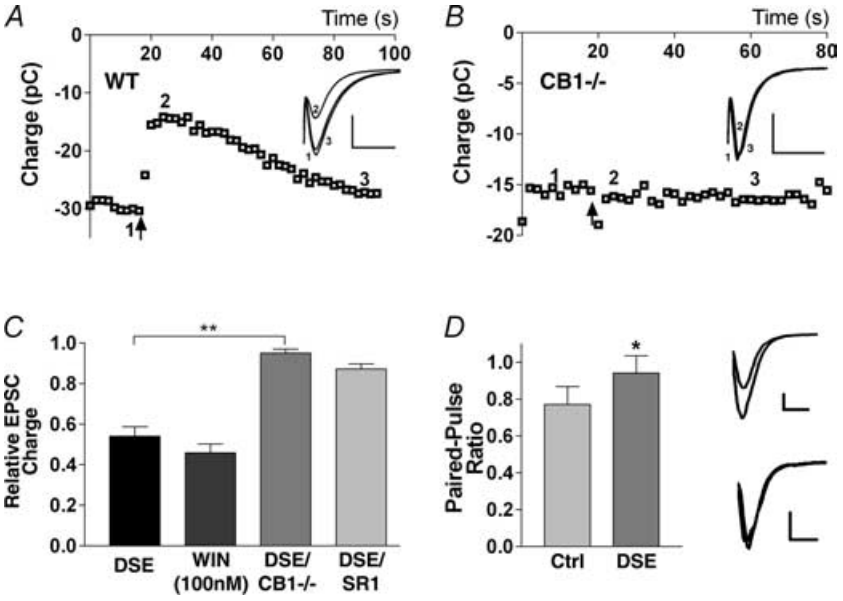

Figure 1. Glutamatergic autaptic hippocampal neurones exhibit DSE
A shows the time course of EPSCs (integral, in pC) recorded before and after depolarizing stimulus (10 s, indicated by arrow) in wild-type (WT) mice. Inset shows relevant traces from time points 1–3 indicated in the main graph (scale bars: 1 nA and 15 ms). *B*, similar recordings performed in cultures from mice lacking the CB1 receptor. Inset as in *A*. *C*, comparison of average inhibitions by DSE stimulus in wild-type neurones, WIN 55212-2 (WIN; 100 nM), DSE stimulus in CB1–/– neurones, and in the presence of the CB1 antagonist SR 141716A (SR1; 100 nM). *D*, left panel shows comparison of paired-pulse ratios before and after DSE stimulus. Right panel shows representative traces (scale bars: 500 pA and 10 ms). $^*P < 0.05$ by Student's paired *t* test; $^{**}P < 0.001$ by one-way ANOVA with Tukey's *post hoc* test.

might explain this variation? It has been proposed that presynaptic cannabinoid sensitivity is a key determinant of the degree of DSE in cultured hippocampal neurones (Ohno-Shosaku *et al.* 2002). In those studies, WIN 55212-2 was found to inhibit EPSCs less (0.43 of control) than IPSCs (< 0.10 of control) and required a higher concentration to do so. For DSE and DSI, in turn, maximal inhibition amounted to ∼0.8 and ∼0.2 of controls, respectively. The autaptic preparation exhibits a similar presynaptic coupling as measured by WIN 55212-2 inhibition of EPSCs (0.46 of control) at a similar concentration (100 nM), but considerably larger DSE (0.54 of control). This suggests that a factor other than presynaptic cannabinoid sensitivity is a determinant of the degree of DSE in autaptic neurones.

In exploring the underpinnings of this difference, we found that cell morphology predicted the degree of DSE. When we compared the degree of DSE inhibition with the ratio of island diameter to soma diameter (a measure of neuronal density/spread), we found that the smaller the ratio, the greater the DSE ($r^2 = 0.64$, $n = 23$; Fig. 3*B*).

Autaptic neurones become so by necessity of the restricted space in which they are allowed to grow and the absence of directly adjoining neighbours. As such, autaptic neurones, particularly those with a highly constrained substrate, begin to grow up, rather than out, and often develop a dense ovoid bundle of processes, as shown schematically in Fig. 3*A*. We found that the ideal morphology of autaptic neurones, for the purpose of observing DSE, was such a dense neuronal bundle.

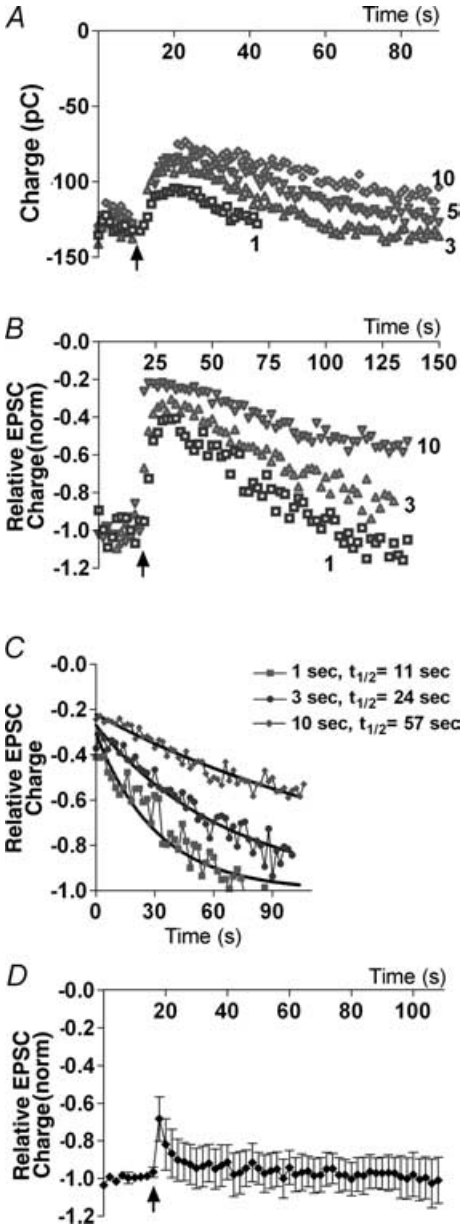

Figure 2. Duration of depolarizing stimulus determines degree of DSE
A, time course of EPSCs recorded before and after DSE stimuli (onset indicated by arrow) of varying durations (1, 3, 5 and 10 s). *B*, time course of EPSCs (normalized to baseline of 1.0 to allow comparison) as in *A*, showing saturation of DSE. *C*, half-life decay time courses ($t_{1/2}$) from same cell, for recovery from DSE. *D*, time course of EPSCs recorded before and after 100 Hz stimulus (duration 2.5 s, onset at arrow).

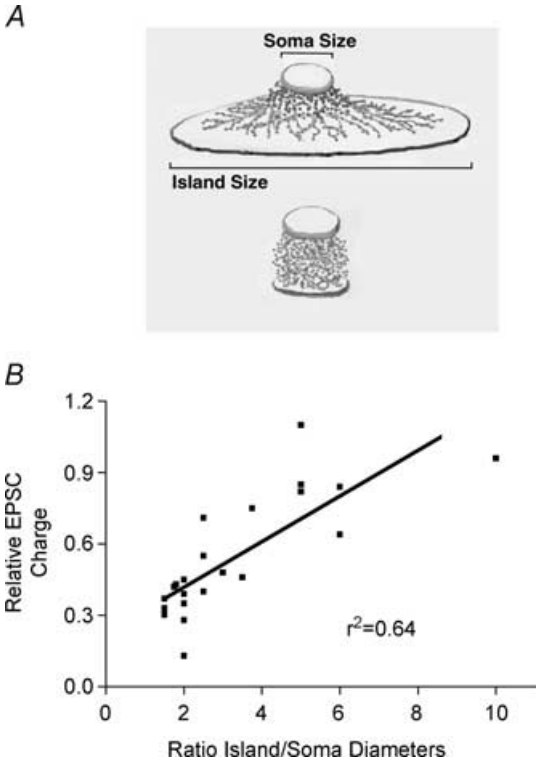

Figure 3. Cell morphology determines extent of DSE
A, schematic drawing showing two autaptic morphologies. Top illustrtion shows the relatively flat configuration of a neurone grown on a larger astrocyte 'island'. Bottom illustration shows a neurone growing on a smaller astrocyte island. *B*, plot of relative EPSC charge *versus* the ratio of island diameter to soma diameter in a given neurone, $r^2 = 0.64$.

While neuronal compactness makes possible greater DSE, exogenous application of the bona fide agonist should strongly inhibit EPSCs regardless of morphology, a subject to which we will return shortly.

Calcium dependence of DSE

DSI has long been known to depend on increased internal postsynaptic calcium (Pitler & Alger, 1992) but there remains uncertainty as to the origin of this calcium, particularly in the case of DSE. Since postsynaptic depolarization is a sufficient stimulus to elicit DSE, calcium influx through voltage-dependent calcium channels (VDCCs) is a promising candidate. To ascertain whether VDCCs are required for DSE, we treated neurones with the non-selective VDCC blocker, cadmium (200 μM), during the depolarizing DSE-eliciting stimulus, washing off the cadmium early and rapidly enough to observe any residual DSE. In control experiments we found that the cadmium inhibition was lifted in about 12 s after commencement of washout, well below the ~60 s duration of DSE.

DSE was only modestly, and often not at all, inhibited by cadmium (DSE after Cd^{2+} washout: 0.70 ± 0.03, control DSE at same time point: 0.66 ± 0.02, $n = 4$; Fig. 4*A*). Since Ca^{2+}-permeable kainate receptors have been reported in hippocampal culture (Ruano *et al.* 1995), and since NMDA receptors might be activated during depolarization, we examined the effect of a similar rapid application protocol with a AMPA/kainate blocker, 6-cyano-7-nitroquinoxaline-2,3-dione (CNQX; 20 μM), and an NMDA blocker, D-aminophosphonovalerate (APV; 50 μM). However, CNQX and APV were without effect on DSE, even in combination (data not shown). Similarly, the sodium channel blocker, TTX (100 μM), did not diminish DSE (data not shown), suggesting that back-propagation of sodium action potentials was not playing a role in eliciting DSE.

Finally, to test whether calcium might derive from internal stores, we pretreated neurones with thapsigargin, a blocker of ER Ca^{2+}-ATPase (Thastrup *et al.* 1990), resulting in an irreversible depletion of internal calcium stores. DSE was attenuated after treatment with thapsigargin (0.86 ± 0.11 of control values, $n = 4$, Fig. 4*B*), indicating that autaptic DSE requires Ca^{2+} release from internal stores.

Endocannabinoids and autaptic DSE

Three candidate endogenous cannabinoids differentially inhibit EPSCs. One of the key unresolved questions in the cannabinoid field concerns the identity of the endogenous cannabinoid(s) (eCB) that activates CB1 receptors. Several candidates have emerged, most prominently anandamide (arachidonyl ethanolamide, or AEA; Devane *et al.* 1992) and 2-arachidonyl glycerol (2-AG; Stella *et al.* 1997). A third candidate eCB, 2-arachidonyl glycerol ether (2-AGE, or noladin ether; Hanus *et al.* 2001; but see Oka *et al.* 2003) has generated some interest and was also included in our study. None of these putative eCBs has been investigated with respect to its ability to inhibit EPSCs in autaptic neurones. Therefore we tested these three candidates to explore their capacity for serving as the endogenous messenger for DSE.

We found that the activity of these candidate endocannabinoids fitted reasonably well with what is known about their activity at the CB1 receptor (Luk *et al.* 2004). 2-AG proved to be both more efficacious and potent than noladin ether, their EC_{50} values were 310 nM and 1.1 μM, and maximal inhibitions to 0.32 and 0.61 of control, respectively (Figs 5*A* and 6*A*). However, EPSCs recovered poorly following treatment with noladin ether, even when the treatment was brief (30–60 s), and even with extended time available for recovery (Fig. 5*A*). This non-reversible inhibition was absent in CB1–/– cultures, indicating that this is a CB1 receptor-dependent phenomenon. AEA inhibited EPSCs only modestly at 450 nM (0.81 ± 0.07, $n = 11$; Fig. 5*B*), a value well above the expected EC_{50} for N-type calcium channel inhibition by AEA (Mackie *et al.* 1993). At 4.5 μM, AEA inhibited EPSCs further (0.62 ± 0.04, $n = 10$). AEA inhibition was also non-reversible (Fig. 5*B*). Inhibition by AEA was absent in CB1–/– cultures (1.03 ± 0.01, $n = 3$; Fig. 5*B*) and was reversed by subsequent application of SR 141716A (100 nM, $n = 3$; Fig. 5*C*). The latter suggests

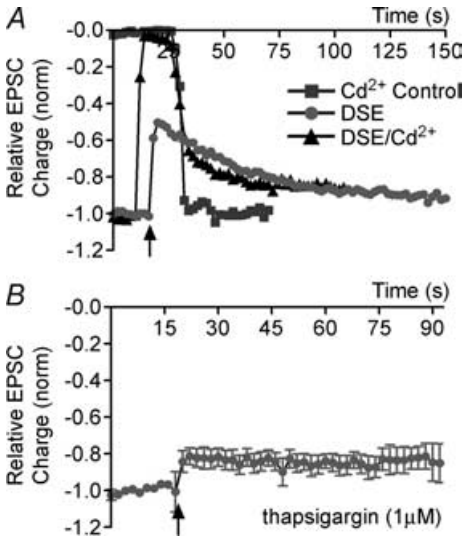

Figure 4. Ca^{2+} dependence of DSE
A, an example of DSE unaffected by Cd^{2+} block. Time course of EPSC size under three conditions: (1) cadmium control; (2) DSE control; and (3) DSE + cadmium. *B*, time courses of DSE (indicated by arrow) after treatment with thapsigargin (1 μM, $\geq$ 20 min).

that the apparent non-reversibility is due to persistent binding.

Non-reversibility of inhibition is inconsistent with status as a bona fide mediator of DSE in these cells since recovery from DSE is rapid and complete. 2-AG, in contrast to both AEA and noladin ether, recovered promptly on washout, with a recovery time course closely approximating that for DSE, even after 20 min of treatment ($t_{1/2} = 41$ s, $n = 7$; Fig. 6*B* and *C*).

Maximal DSE inhibition *versus* same-cell eCB inhibition. Exogenous application of a saturating concentration of an eCB that causes DSE should result in a maximal inhibition equal to or greater than seen with DSE. It has not been possible to perform this experiment usefully in conventional cultures, mainly because of polycell network considerations. In the autaptic preparation, however, we may be confident that all eCB release derives from a single neurone. Having defined saturating maximal inhibition by DSE in a given cell, we may thus usefully compare this to the maximal inhibition by an agonist of choice. Furthermore, given what we have learned about morphological determinants of maximal DSE inhibition, one would predict that exogenous treatment with the bona fide eCB would always produce a high degree of inhibition that would be matched by DSE inhibition only in the most tightly packed neurones.

Both noladin ether and AEA yielded an average inhibition comparable to that for DSE in same-cell experiments (noladin ether: 0.61 *versus* 0.56 of control value; AEA: 0.61 *versus* 0.54 of control value; Fig. 5*A* and *B*). However, DSE inhibition exceeded that elicited by 10 μM noladin ether in six of nine cells tested (and 1 of 2 cells treated with 50 μM noladin ether). Thus, for noladin ether to routinely exceed DSE inhibition would require concentrations in the physiologically unlikely ≥ 100 μM range. A similar situation prevailed for AEA; DSE inhibition exceeded that for 4.5 μM AEA in several cells tested.

In contrast, 2-AG produced a maximal inhibition that considerably exceeded that for DSE on average (0.32 *versus* 0.51 with same-cell control) in nearly every cell tested. Thus the degree of 2-AG inhibition was independent of cell geometry and correlated very weakly with DSE inhibition ($r^2 = 0.09$, $n = 11$; Fig. 6*D*). DSE inhibition approached that for 2-AG only in cells with the smallest island : soma diameter ratios.

That 2-AG exceeds maximal DSE inhibition fits nicely with the above morphological/DSE observations and is consistent with the explanation that endogenously

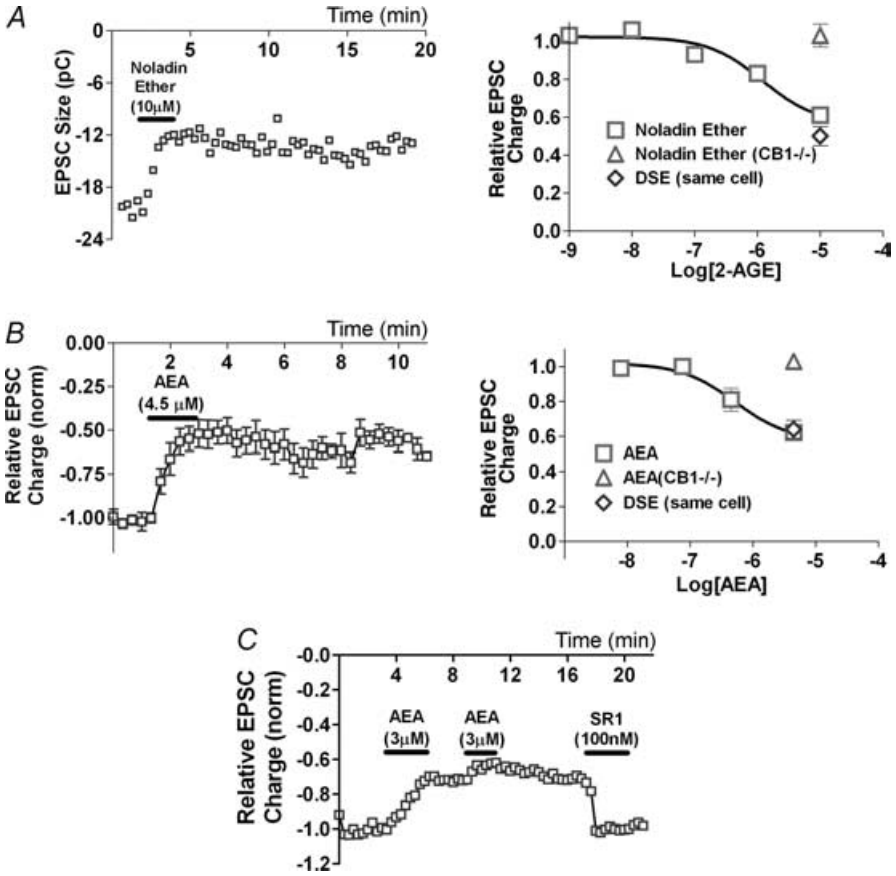

Figure 5. AEA and noladin ether inhibit EPSCs with poor reversibility
A, left panel shows sample time course of EPSC size in response to noladin ether treatment (10 μM). Right panel shows dose–response curve for noladin ether in wild-type neurones (□, $n = 2$–10). △, noladin ether in CB1–/– neurones ($n = 4$); ◇, DSE inhibition in neurones subsequently treated with 10 μM noladin ether ($n = 11$). *B*, left panel shows summary time course of EPSC size (pC) in neurones treated with AEA (4.5 μM). Right panel shows dose–response curve for AEA in wild-type neurones (□, $n = 3$–11). △, AEA in CB1–/– neurones ($n = 3$); ◇, DSE inhibition in neurones subsequently treated with 4.5 μM AEA ($n = 11$). *C*, time course of neurone treated with AEA (3 μM), then with SR 141716A (100 nM).

produced eCBs do not reach all available receptors, even with favourable autaptic morphology and despite saturating DSE. Furthermore, one would predict 2-AG occlusion of DSE only at a concentration that produces an inhibition comparable to the maximal DSE inhibition seen under favourable conditions (i.e. 5 μM 2-AG). Indeed, in occlusion experiments where DSE was elicited first in the absence and then in the presence of 2-AG, we found that 2-AG did not significantly occlude DSE at 500 nM (DSE/2-AG: 0.57 ± 0.05 *versus* DSE control in same cell: 0.44 ± 0.07, $n = 6$), the concentration at which 2-AG inhibition matched the average DSE inhibition, whereas the maximally inhibiting 5 μM 2-AG completely occluded DSE (1.07 ± 0.04 of control value, $n = 4$; Fig. 6*E*).

Pharmacology of autaptic DSE

Of the three candidate eCBs examined with respect to their inhibition of EPSCs, only 2-AG exhibits a profile consistent with DSE. If 2-AG is indeed the eCB mediating DSE in these neurones, one would expect a distinct pattern of eCB pharmacology. A variety of proteins are known (or suspected) to play roles in synthesizing, breaking down and transporting one or another of these candidate eCBs.

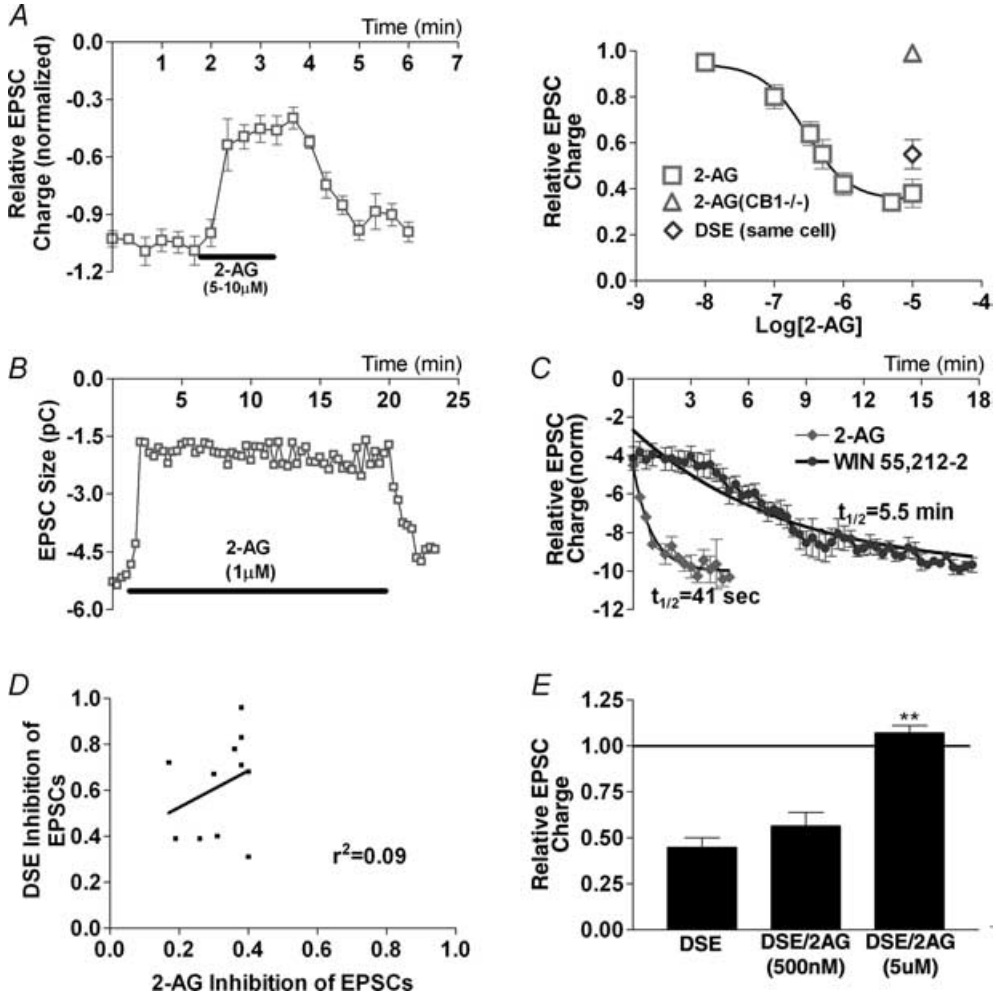

Figure 6. 2-AG action closely mimics DSE
A, left panel shows summary time course of EPSC size (normalized) in neurones treated with 2-AG (5–10 μM). Right panel shows dose–response curve for 2-AG in wild-type neurones (□). △, 2-AG in CB1–/– neurones; ◇, DSE inhibition in neurones subsequently treated with 1–10 μM 2-AG. *B*, sample time course of EPSC inhibition during long-term 2-AG treatment (1 μM). *C*, decay time course for recovery from 2-AG treatment (1–10 μM). Recovery time course for WIN 55212-2 (100 nM) is included for comparison. *D*, plot of DSE *versus* 2-AG (5–10 μM) inhibition of EPSCs; $r^2 = 0.09$. *E*, comparison of EPSC inhibition by DSE alone and DSE in the presence of 500 nM and 5 μM 2-AG. $^{**}P < 0.005$ by Student's paired *t* test.

For example, the fatty acid amidohydrolase is thought to break down AEA but not 2-AG *in vivo*, whereas monoacylglycerol lipase is thought to hydrolyse 2-AG, but not AEA.

eCB synthesis

DAG lipase. 2-AG (but not AEA) can be produced via hydrolysis of 1,2-diacylglycerol (DAG) by *sn*-1-diacylglycerol lipase (Bisogno *et al.* 2003). If 2-AG were the endogenous ligand mediating autaptic DSE, one would expect inhibition of DAG lipase to diminish DSE. Consistent with this, we found that treatment (10 min) with the DAG lipase inhibitor, RHC-80267 (30 μM), substantially attenuated DSE (same-cell control: 0.50 ± 0.06; RHC: 0.71 ± 0.08, $n = 8$; Fig. 7*A*).

DAG kinase inhibitor 1. As mentioned above, 2-AG production is expected to occur via the action of DAG lipase. The pool of available DAG may be modulated by the activity of DAG kinase, which phosphorylates DAG, producing phosphatidic acid and effectively shunting DAG down another metabolic pathway, decreasing 2-AG by eliminating its precursor (Topham & Prescott, 2002). Inhibiting DAG kinase might serve to increase the available DAG and perhaps, ultimately, 2-AG (Franklin & Stella, 2003; Witting *et al.* 2004), effectively amplifying DSE. To explore this possibility, we tested DAG kinase inhibitor 1 (DAGKI 1). However, at 30 μM, DAGKI 1 completely eliminated EPSCs, even in CB1–/– cultures (data not shown), making DSE measurement unfeasible.

eCB breakdown

AEA breakdown: fatty acid amidohydrolase (FAAH). Fatty acid amidohydrolase (FAAH) is thought to be responsible for the *in vivo* breakdown of AEA (and not 2-AG; Kathuria *et al.* 2003; Lichtman *et al.* 2004). If AEA were a bona fide eCB mediating DSE in these neurones, one would expect inhibition of FAAH to result in an increased maximal inhibition and/or slowed recovery with DSE. We found that the selective FAAH antagonist, URB-597 (100 nM), was without effect on either the maximal extent of DSE inhibition (control: 0.57 ± 0.08; URB597: 0.63 ± 0.05, $n = 6$; Fig. 7*B*) or on the time course of recovery ($t_{1/2}$ control = 30 s; $t_{1/2}$ URB597 = 29 s).

We additionally recorded from neurones cultured from mice lacking the FAAH enzyme. After determining that the WIN 55212-2 dose–responses and DSE responses are the same for C57/Bl6 and CD1 mice (data not shown), we found that FAAH–/– neurones exhibit DSE comparable in degree to that of wild-type neurones (DSE: 0.56 ± 0.06, $n = 13$; Fig. 7*C*). Because the duration of depolarization needed to produce a maximal DSE inhibition varied considerably from cell to cell, one must exercise caution in interpreting decay time course data across populations of neurones. However, the average decay $t_{1/2}$ was similar to the corresponding value for wild-type DSE (FAAH–/–: $t_{1/2} = 29$ s, $n = 7$, *versus* 38 s in FAAH+/+, $P > 0.05$). In principle, FAAH is capable of breaking down 2-AG, and thus might be responsible for at least part of the rapid recovery of EPSCs after removal of exogenously applied 2-AG. However, when FAAH–/– neurones were treated with 2-AG (1–10 μM), the time course of subsequent recovery was unaltered (Fig. 7*D*). These data, taken together, show that FAAH does not appear to shape DSE in these neurones.

COX-2. COX-2 inhibitors have recently been implicated in modulation of DSI in hippocampal pyramidal cells (Kim & Alger, 2004). These investigators reported that COX-2 inhibitors prolonged the recovery from DSI (by ~200%), whereas the FAAH inhibitor URB-597 did not. If COX-2 played a similar role for DSE, one would expect COX-2 inhibition either to prolong DSE recovery or to increase the degree of DSE inhibition. We found in same-cell experiments that treatment with the COX-2 inhibitor, nimesulide (30 μM), for 10 min did not significantly affect maximal inhibition (DSE control: 0.56 ± 0.05; DSE with nimesulide in same cell: 0.62 ± 0.06, $n = 8$, $P > 0.05$; Fig. 7*E*), and did not significantly extend the recovery half-life ($t_{1/2}$ control = 48 s; $t_{1/2}$ nimesulide = 62 s, $P > 0.05$).

The endocannabinoid membrane transporter

The existence of an endocannabinoid membrane transporter (EMT) has been postulated, although its precise role and the protein(s) mediating this process remain to be identified. For instance, does the transporter serve primarily to remove residual endocannabinoids from the synaptic environment (Beltramo *et al.* 1997; Bisogno *et al.* 2001), or to regulate eCB release itself (e.g. Ronesi *et al.* 2004), or both? The transporter appears to act via facilitated diffusion. Thus transport should be possible in both directions with eCB flux down its concentration gradient.

The autaptic preparation is well suited to examine this question, since one can study both single-source release and the rate of uptake. If the EMT acts to clear eCBs from the synapse/presynaptic membrane, one would expect an endocannabinoid transport inhibitor (ETI) to slow the recovery rate for both DSE and exogenously applied eCBs. If, instead, the principal role of the transporter is to deliver eCBs into the synapse, one would expect an ETI to inhibit DSE itself.

To explore this question we employed the relatively potent and selective ETI, UCM-707 (Lopez-Rodriguez

et al. 2003*a*,*b*). Bath application of UCM-707 (8–10 μM) substantially inhibited DSE (control DSE inhibition: 0.45 ± 0.05; DSE inhibition in the presence of UCM-707: 0.83 ± 0.02, $n = 3$; Fig. 8*A*) without affecting EPSC size (Fig. 8*B*). The reduced DSE following UCM-707 rendered reliable calculation of DSE recovery difficult. However, if UCM-707 inhibits uptake, this might also affect the rapid recovery from exogenous 2-AG application. To test

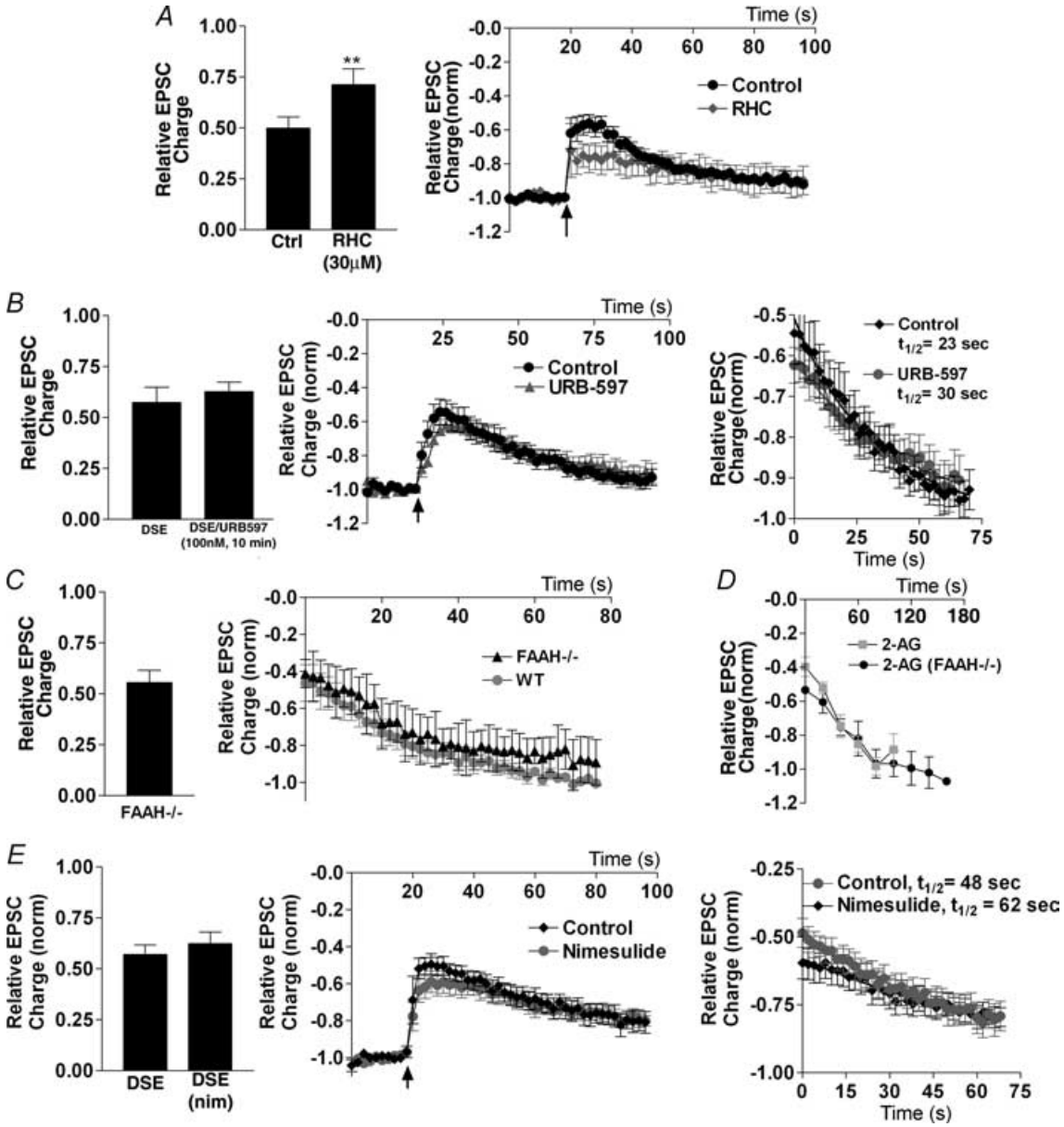

Figure 7. Endocannabinoid production and breakdown
A, left panel shows DSE inhibition in neurones before and after 10 min in RHC-80267 (30 μM). Centre panel shows averaged normalized time courses of EPSC inhibition by DSE protocol (indicated by arrow) in control and RHC-80267-treated conditions. *B*, left panel shows comparison of DSE inhibition in neurones before and after 10 min in URB-597 (100 nM). Centre panel shows averaged normalized time courses of EPSC inhibition by DSE protocol (indicated by arrow) in control and URB-597-treated conditions. Right panel shows decay time course after DSE stimulation in the same cells under control and URB-597-treated conditions. *C*, left panel shows DSE inhibition of EPSCs in neurones cultured from FAAH–/– mice. Right panel shows averaged time courses of recovery of EPSC after DSE stimulus in FAAH–/– and FAAH+/+ neurones. *D*, time courses of recovery from EPSC inhibition by 2-AG in FAAH–/– and FAAH+/+ neurones. *E*, left panel shows comparison of DSE inhibition in neurones before and after 10 min in nimesulide (30 μM). Centre panel shows averaged normalized time courses of EPSC inhibition by DSE protocol (indicated by arrow) in control and nimesulide-treated conditions. Right panel shows decay time course after DSE stimulation in the same cells under control and nimesulide-treated conditions. $^{**}P < 0.005$ by Student's paired *t* test.

this we treated cells with 2-AG (10 μM) followed by a 10 min treatment with UCM-707 and a subsequent coapplication of UCM-707 and 2-AG (Fig. 8*B* and *C*). UCM-707 treatment had no effect on the degree of inhibition by 2-AG (thus also confirming that UCM-707 does not directly inhibit (or activate) CB1 receptors; 2-AG: 0.52 ± 0.04 2-AG with UCM-707: 0.57 ± 0.12, $n = 4$; Fig. 8*C*). UCM-707 treatment did not change the time course of recovery following 2-AG treatment (Fig. 8*C*). We also included UCM-707 in our internal recording solution, recording an initial DSE series followed by another set after 10 min. This resulted in only a very slight (though statistically significant, $P = 0.01$) decrease in DSE (Fig. 8*D* and *E*) and no effect on the recovery time course.

The inhibition of DSE by an ETI suggests that: (1) a functional endocannabinoid transporter is present in these neurones; and (2) this transporter plays a role in eCB release but not in clearance/uptake.

Additional DSE-related pharmacology

It has been suggested that brain-derived neurotrophic factor (BDNF) may be a mediator of CB1 receptor-dependent neuroprotection (Marsicano *et al.* 2003). Since there are reports of BDNF modulation of neurotransmission in the hippocampus (reviewed by Lu, 2003), we examined whether BDNF affected DSE in our cultures. We found that treatment with BDNF (0.2 μg ml^{-1},

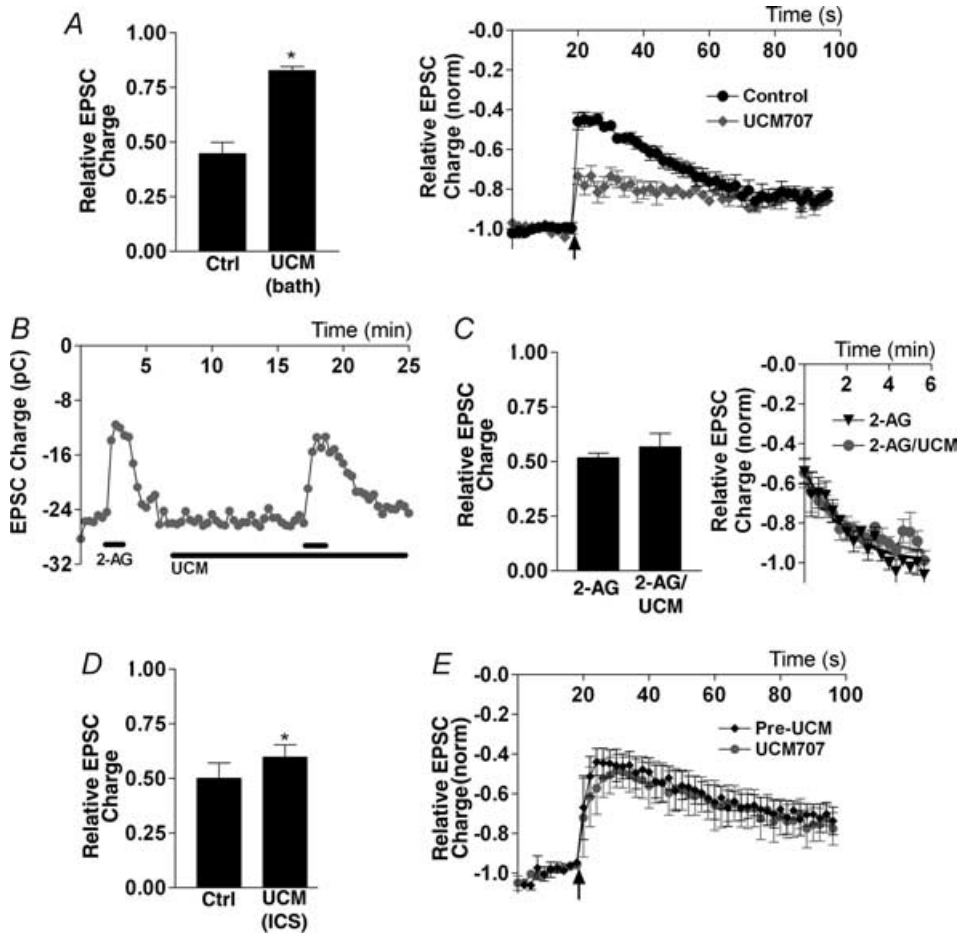

Figure 8. The endocannabinoid membrane transporter is required for DSE but not for endocannabinoid uptake

A, left panel shows comparison of DSE inhibition in neurones before and after treatment with UCM-707 (8–10 μM, bath applied for 10 min). Right panel shows averaged normalized time courses of EPSC inhibition by DSE protocol (indicated by arrow) in control and UCM-707-treated conditions. *B*, time course of EPSCs in response to 2-AG (1 μM) alone, and after UCM-707 treatment (8 μM). *C*, left panel shows summary of same-cell inhibition with 2-AG *versus* 2-AG with/after 10 min of treatment with UCM-707. Right panel shows averaged recovery time courses of 2-AG before and after UCM-707 treatment. *D*, left panel shows comparison of DSE in neurones before and after 10 min with UCM-707 (8–10 μM) in the internal pipette solution (intracellular solution, ICS). Right panel shows averaged normalized time courses of EPSC inhibition by DSE protocol (indicated by arrow) in control and UCM-707-treated conditions. $^*P < 0.05$ by Student's paired *t* test.

10 min) had no effect on EPSC size (data not shown) or on DSE inhibition (DSE: 0.58 ± 0.09; BDNF: 0.63 ± 0.05, $P > 0.05$, $n = 3$).

Insulin is an additional receptor tyrosine kinase known to be active in cultured hippocampal neurones where it has been shown to potentiate μ opioid receptor activation (McLaughlin & Chavkin, 2001). We investigated potential effects on EPSCs and DSE and found that while a high concentration of insulin (8 μM) rapidly and reversibly potentiated EPSCs to a small but significant degree (1.19 ± 0.04, $P < 0.005$, $n = 7$), this effect did not alter WIN 55212-2 inhibition, even with 10 min insulin treatment (first WIN 55212-2, 100 nM: 0.44 ± 0.03; second WIN 55212-2, 10 min postinsulin: 0.49 ± 0.04, $P > 0.05$, $n = 8$). Nor did insulin treatment affect DSE (first DSE: 0.52 ± 0.09; DSE with 8 μM insulin for 10 min: 0.60 ± 0.10, $P > 0.05$, $n = 8$).

To explore (or rule out) a possible role for vanilloid receptors, we treated neurones with the vanilloid receptor agonist capsaicin. EPSCs and holding current were closely monitored upon treatment with capsaicin (300 nM), but no effect was observed on EPSCs or holding current (data not shown), suggesting that the TRPV1 receptors are not present in this preparation and thus cannot participate in DSE.

Astrocytes and eCB synthesis. Cultured autaptic neurones are grown on a feeder layer of astrocytes. In principle, these astrocytes might play a role in DSE. It has been shown, for instance, that endothelin-1 can induce the release of 2-AG from cultured astrocytes (Walter & Stella, 2003). Can endothelin elicit eCB release from astrocytes in autaptic cultures sufficient to inhibit EPSCs in the neurones they are nourishing? It appears not, since 100 nM endothelin had no effect on EPSC size (data not shown) or on DSE (1.0 ± 0.01, $n = 3$).

We have observed that a larger astrocyte island base (consisting of more astrocytes; data not shown) correlates with diminished, rather than enhanced, DSE. The lack of effect of endothelin does not rule out 2-AG release from these astrocytes, but taken together with the above morphology/DSE observation, suggests that astrocytes are unlikely to explain or even extensively modulate the DSE observed in autaptic neurones.

Nitric oxide and DSE. DSE is known to require postsynaptic depolarization but presynaptic CB1 receptor activation, and therefore a retrograde messenger, one commonly assumed to be an eCB, is necessary. However, all putative eCBs are membrane-preferring lipids and, as such, would seem to be poor candidates as synaptic cleft-traversing neurotransmitters. In principle, another neurotransmitter (nitric oxide is often mentioned) might serve the trans-synaptic role, crossing the cleft to elicit presynaptic production of eCBs. To determine whether nitric oxide might play such a role in autaptic neurones, we treated them with the non-selective nitric oxide synthase inhibitor, L-NAME (50 μM). A 10 min treatment with L-NAME had no effect on EPSC size (data not shown) or on DSE (first DSE: 0.61 ± 0.09; DSE in same cell after 10 min L-NAME treatment: 0.59 ± 0.14, $n = 4$), indicating that nitric oxide is unlikely to mediate DSE in this preparation.

Δ^9-THC and autaptic DSE

As evidence has accumulated that endocannabinoid-mediated synaptic plasticity represents a primary manifestation of the endocannabinoid signalling system, the question of how the principal psychoactive ingredient of marijuana, Δ^9-THC (Gaoni & Mechoulam, 1964), interacts with that system is of great interest and consequence. Like AEA, Δ^9-THC is known to be a partial agonist at the CB1 receptor. Thus one would expect Δ^9-THC to inhibit EPSCs in a fashion similar to AEA. Remarkably, however, we found that Δ^9-THC does not inhibit EPSCs at all, even at concentrations exceeding 10 μM (Fig. 9*A* and *B*) and when treatments were extended to 10 min (data not shown). Yet 600 nM Δ^9-THC was sufficient to prevent EPSC inhibition by the synthetic agonist WIN 55212-2 (100 nM; 0.84 ± 0.05, $n = 5$; Fig. 9*D*). Furthermore, 600 nM Δ^9-THC attenuated, and 6 μM Δ^9-THC occluded, DSE (600 nM Δ^9-THC: 0.63 ± 0.07, $n = 6$; 6 μM Δ^9-THC: 0.83 ± 0.04, $n = 3$; Fig. 9*C* and *D*). These results attest to the effectiveness of the Δ^9-THC in our preparation and indicate that the failure to inhibit EPSCs was not due to lack of penetration and/or Δ^9-THC–receptor interaction. Thus Δ^9-THC antagonizes both exogenous and endogenous activation of the CB1 receptor.

Interestingly, in cultures that were treated with Δ^9-THC overnight (~18 h, 450 nM Δ^9-THC followed by 20 min wash), Δ9-THC also eliminated the WIN 55212-2 (100 nM) response (0.98 ± 0.03, $n = 4$; Fig. 10*A*) and the DSE response (0.91 ± 0.07, $n = 4$; Fig. 10*B*), in an apparent desensitization (Sim *et al.* 1996; Breivogel *et al.* 1999; Bass & Martin, 2000). To rule out the possibility that this observation is instead due to receptor occupation/membrane saturation by Δ^9-THC, we treated Δ^9-THC-desensitized neurones with 100 nM HU-210, a high-affinity CB1 receptor agonist that inhibits EPSCs in the presence of 450 nM Δ^9-THC (0.60, $n = 2$; Fig. 10*C* and *E*). HU-210 showed no effect in Δ^9-THC-desensitized neurones (1.09, $n = 3$; Fig. 10*D* and *E*). Thus it may be concluded that Δ^9-THC antagonizes CB1 receptors in the short term but desensitizes them in the long term. Such a relationship may have considerable implications for Δ^9-THC action *in vivo*.

Discussion

DSE was observed in cultured autaptic hippocampal neurones, thereby demonstrating that a single neurone may functionally express both the pre- and postsynaptic components of retrograde eCB signalling. This simple preparation opens a new avenue for the study of retrograde eCB signalling, particularly that of the relatively elusive hippocampal DSE.

eCBs and DSE

Taken together, our experiments involving bath application of putative eCBs leave 2-AG as the only principal candidate eCB standing, and therefore promote 2-AG as the mediator of DSE in this preparation. If 2-AG is indeed the bona fide cannabinoid here, the local concentration of 2-AG under saturating DSE conditions may be calculated at $\sim$5 μM. The apparent non-reversibility of AEA and noladin ether may simply be a matter of slow clearance of these lipids from the cell membrane. At 100 nM the synthetic agonist WIN 55212-2 (also lipophilic) washes out slowly ($t_{1/2} = \sim$5 min). Higher WIN 55212-2 concentrations, approaching those used for AEA and noladin ether, result in recovery times that are slower still. Given the gross structural similarities between 2-AG, 2-AGE and AEA, a parsimonious explanation for the rapid recovery of 2-AG is the action of a selective and active clearance mechanism. That mechanism does not appear to require the EMT, FAAH or COX-2.

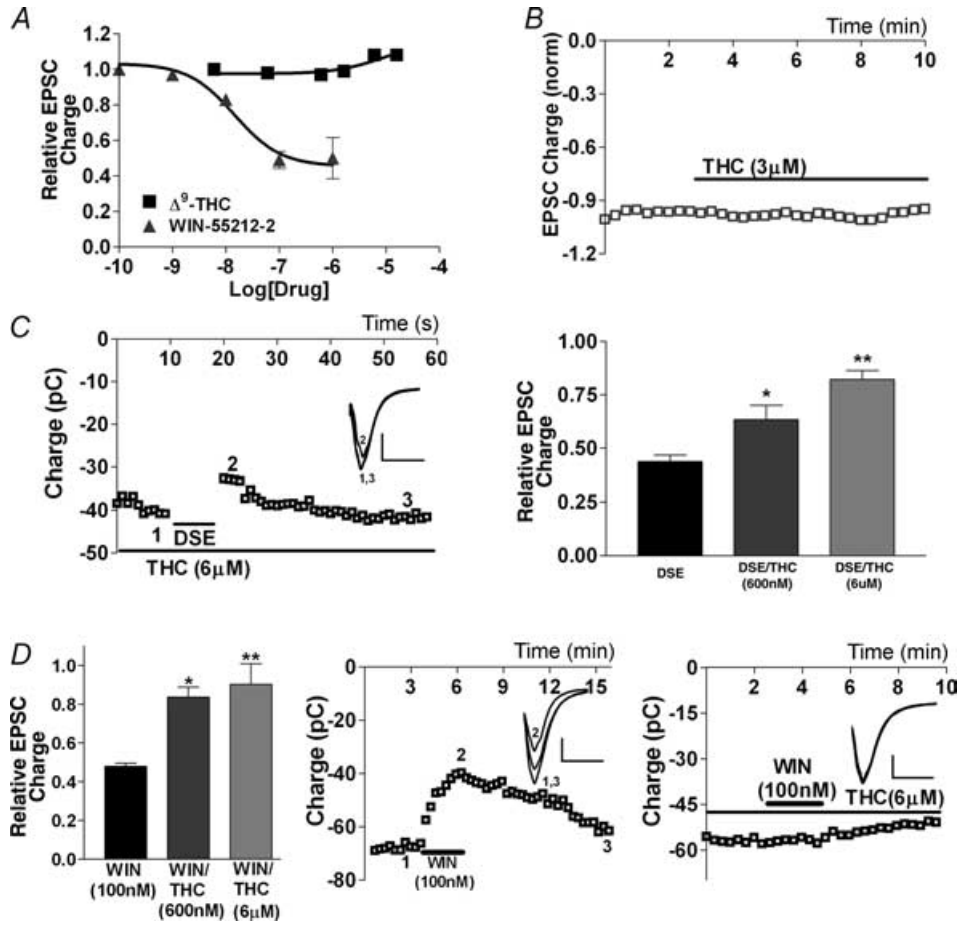

Figure 9. Δ^9-THC does not inhibit EPSCs, but occludes DSE and WIN 55212-2 inhibition
A, dose–response curves for Δ^9-THC ($n = 5$–10) and WIN 55212-2 ($n = 3$–10) inhibition of EPSCs. *B*, plot of the time course of EPSC size (in pC) in response to treatment with Δ^9-THC (3 μM). *C*, left panel shows a sample time course of EPSC inhibition in response to DSE protocol in the presence of Δ^9-THC (6 μM). Inset shows sample EPSC traces at time points indicated in left-hand panel (1–3). Right panel shows comparison of DSE inhibition in the absence and presence of Δ^9-THC (600 nM and 6 μM). *D*, left panel shows comparison of WIN 55212-2 (100 nM) inhibition on its own and in the presence of Δ^9-THC (600 nM and 6 μM). Centre and right panels show sample time courses of EPSC inhibition by WIN 55212-2 in the absence and presence of 6 μM THC, respectively. Insets show corresponding EPSC traces at time points labelled in the main panels. $^*P < 0.05$, $^{**}P < 0.01$ by Student's *t* test.

Δ^9-THC and DSE

Δ^9-THC is known to be a partial agonist at the CB1 receptor (Sim *et al.* 1996; Shen & Thayer, 1998; Luk *et al.* 2004). Still, one would expect the chief psychoactive ingredient of marijuana to have some inhibitory effect on EPSCs, particularly since Δ^9-THC in hippocampal cultures caused a ∼20% reduction in calcium spiking frequency (Kelley & Thayer, 2004*b*). Δ^9-THC is clearly effective in our preparation, since it readily occludes both DSE and WIN 55212-2 inhibition and desensitizes the CB1 receptor, yet Δ^9-THC has no discernible effect on EPSCs. The lack of EPSC inhibition may be a function of low receptor density combined with poor efficacy in coupling with downstream effectors when activated by Δ^9-THC.

Perhaps even more interesting than the non-inhibition of EPSCs is the clear occlusion of both exogenous and endogenous CB1 receptor activation over the short term, coupled with elimination of CB1 responses over the long term (desensitization). Both of these actions will result in functional antagonism of the CB1 receptor signalling system. Our observations, together with other recent reports (Kelley & Thayer, 2004*b*; Mato *et al.* 2004), lead to a provocative concept regarding the role of the interaction of Δ^9-THC with the endogenous cannabinoid system in what appears to be a major role in the brain. Does Δ^9-THC

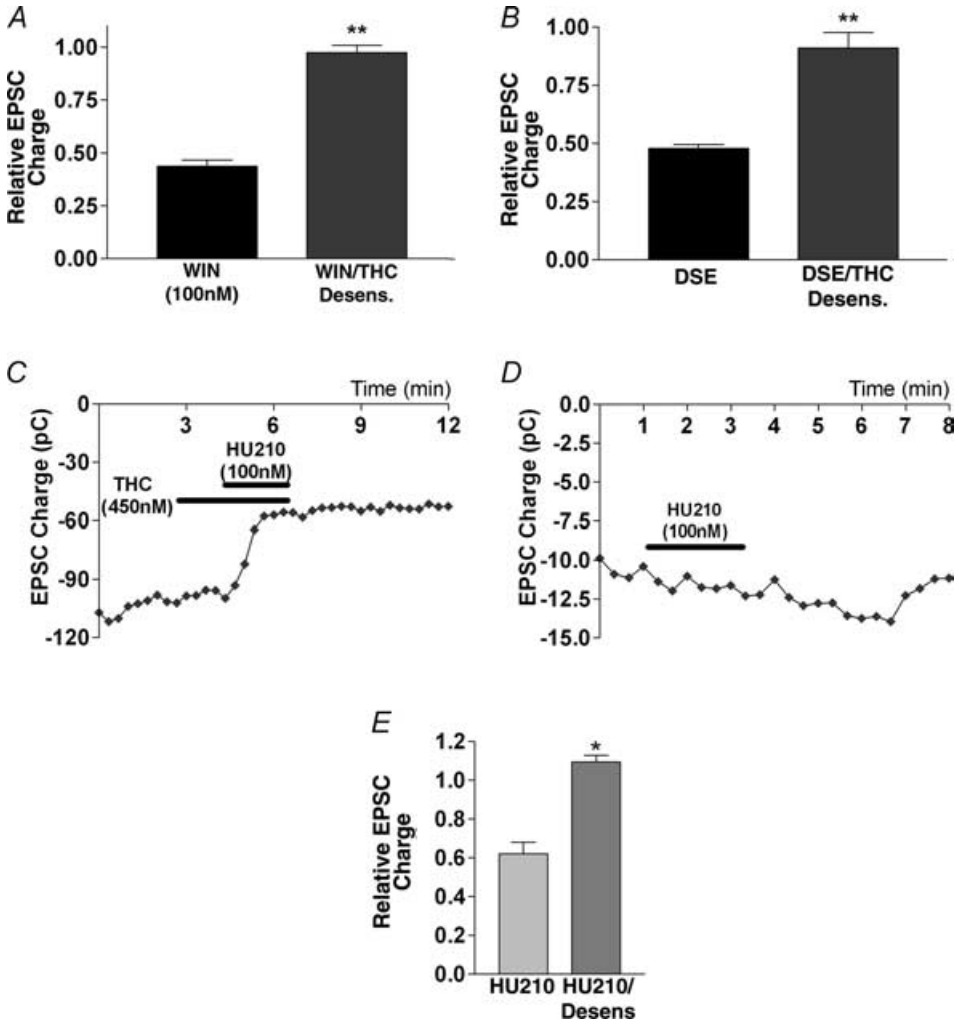

Figure 10. Δ^9-THC desensitizes CB1 receptors
A, comparison of inhibition by WIN 55212-2 of EPSCs in control and Δ^9-THC-treated neurones (450 nM for 19 h, followed by ≥ 20 min washout). *B*, comparison of DSE in control and Δ^9-THC-treated neurones (as in *A*). *C*, sample time course of EPSCs in response to treatment with Δ^9-THC alone (450 nM) and in combination with HU-210 (100 nM). *D*, sample time course of EPSCs in response to treatment with HU-210 in Δ^9-THC-treated neurones (450 nM for 19 h, ≥ 20 min washout). *E*, summary of treatments with HU-210 in the presence of Δ^9-THC and HU-210 in Δ^9-THC-desensitized neurones. $^*P < 0.05$, $^{**}P < 0.005$ by Student's *t* test.

act in the brain chiefly by inhibiting existing endogenous signalling? Such a role would stand in considerable contrast to what has generally been assumed.

Mechanism and determinants of DSE

Autaptic cultured murine hippocampal neurones express many receptors, channels and signalling pathways, and make possible the isolated study of individual neurone types within a larger population without the constraints of conventionally cultured neuronal networks. Autaptic neurones are ultimately a simple system; this being both the basis of their attraction and a reason for circumspection in relating the present results to *in vivo* cannabinoid function. In some cases this is simply a matter of considering the experimental conditions; for instance, the time courses of DSI and DSE recovery have been found to be sensitive to temperature (the time course of cerebellar DSE decreases from ∼15 to ∼10 s at temperatures of 24 and 34°C, respectively; Kreitzer *et al.* 2002). DSE recovery times in autaptic hippocampal neurones would no doubt be more rapid at higher temperatures.

In other instances, findings from autaptic neurones may be less easily reconciled with *in vivo* function. For example, is the finding that cell geometry predicts the degree of DSE likely to be unique to the preparation? The greater inhibition in densely plated cultures may be due to glutamate spillover and activation of extrasynaptic mGluR receptors as has recently been described (Marcaggi & Attwell, 2005) in the cerebellum, or may simply occur because eCBs do not reach all available receptors in cells with a larger island:soma diameter ratio. In the latter instance, favourable autaptic morphology would promote more robust DSE by directly juxtaposing a greater share of presynaptic terminals with presumed somatodendritic eCB release sites. In keeping with both arrangements, we found that the candidate eCB, 2-AG, robustly inhibited EPSCs regardless of neuronal morphology. In this limited respect, autaptic culture may occupy a middle ground between the flat bath-exposed neurones of conventional culture on the one hand and neurones in slice preparations on the other.

Our results have some bearing on an on-going debate concerning the identity of the cannabinoid receptor in hippocampal excitatory transmission. Hajos *et al.* (2001) reported inhibition of excitatory transmission by the agonist WIN 55212-2 in the absence of CB1 receptors, raising the possibility of an additional cannabinoid receptor. Subsequently, Ohno-Shosaku *et al.* (2002) published a contrary result, albeit one that may be explained by their use of cultured neurones from mice of a different strain. Our results in cultured neurones clearly fit with the latter study (though we use the same mouse strain as Hajos *et al.* 2001), while adding a more robust DSE. But how are the several published reports of CB1-dependent modulation of excitatory hippocampal transmission (Sullivan, 1999; Ameri & Simmet, 2000; Ohno-Shosaku *et al.* 2002) to be reconciled with evidence against the presence of CB1 receptors in excitatory terminals (Hajos *et al.* 2000; Katona *et al.* 2000)? It is too soon to explain this seeming contradiction or even to say whether it is a contradiction. What is clear is that excitatory hippocampal neurones can produce CB1 receptors and possibly additional putative cannabinoid receptor(s).

The presynaptic mechanism of autaptic hippocampal DSE probably occurs in a manner similar to what has been detailed for WIN 55212-2-induced inhibition of presynaptic glutamate release in rat autaptic hippocampal culture (Sullivan, 1999). On the postsynaptic end, while it is known that DSI and DSE depend on a postsynaptic rise in calcium, that calcium could arise from outside via ion channels and/or from internal stores. For DSE this question is essentially unexplored. We determined that DSE can occur in the face of a VDCC blockade and that DSE is much diminished after treatment with the Ca^{2+}-ATPase blocker, thapsigargin. Thus a major source of calcium for autaptic DSE appears to derive from internal calcium stores, a result that differs considerably from what is generally believed to occur with DSI. It should, however, be noted that in slices it can be difficult to dissect pre- from postsynaptic external calcium dependence; for instance, the oft-cited report of Lenz *et al.* (1998) was unable to distinguish between the two (Alger, 2002). There is other evidence for DSI dependence on VDCCs, notably a study that used rapid wash-on and wash-off of 0 M Ca^{2+} in hippocampal cultures (Ohno-Shosaku *et al.* 1997), but a recent investigation of DSI in the dentate gyrus (Isokawa & Alger, 2005) clearly shows a dependence on internal stores and indicates that the question of origin of postsynaptic calcium for DSI, considered by many to be resolved, may deserve some revisiting and reappraisal.

Bath application of the EMT inhibitor, UCM-707, diminishes DSE, implying a postsynaptic EMT with a key role in eCB release, a function that has previously been proposed in the striatum (Ronesi *et al.* 2004). In contrast to the report by Ronesi and colleagues, intracellular application of the EMT inhibitor resulted in only a very modest inhibition of DSE. This may be explained by a rapid absorption of the lipophilic UCM-707 into the membrane, resulting either in local partitioning away from the eCB release site or diffusion out of the neurone before it can reach its target. The EMT does not account for the rapid recovery from DSE or exogenously applied 2-AG and therefore does not appear to play a role in eCB clearance under these conditions.

DSE is likely to take diverse forms in different brain regions and perhaps during development, having adapted to fit the numerous needs of neuronal signalling in various regions of the brain at different times. Dissecting and characterizing the components of functional autaptic DSE,

particularly with respect to identification of 2-AG as the likely eCB, the interaction with Δ^9-THC, the role of the EMT and the calcium dependence, has delivered several substantive insights to cannabinoid signalling. Thus autaptic DSE adds a promising new tool for high-resolution study of the molecular underpinnings of DSE in particular and for cannabinoid signalling in general. If, additionally, it proves possible to observe cannabinoid-dependent retrograde signalling in autaptic neurones cultured from other regions of the brain, this may greatly facilitate the study of cannabinoid action throughout the brain.

References

Alger BE (2002). Retrograde signaling in the regulation of synaptic transmission: focus on endocannabinoids. *Prog Neurobiol* **68**, 247–286.

Ameri A & Simmet T (2000). Effects of 2-arachidonylglycerol, an endogenous cannabinoid, on neuronal activity in rat hippocampal slices. *Naunyn Schmiedebergs Arch Pharmacol* **361**, 265–272.

Bass CE & Martin BR (2000). Time course for the induction and maintenance of tolerance to Delta(9)-tetrahydrocannabinol in mice. *Drug Alcohol Depend* **60**, 113–119.

Bekkers JM & Stevens CF (1991). Excitatory and inhibitory autaptic currents in isolated hippocampal neurons maintained in cell culture. *Proc Natl Acad Sci U S A* **88**, 7834–7838.

Beltramo M, Stella N, Calignano A, Lin SY, Makriyannis A & Piomelli D (1997). Functional role of high-affinity anandamide transport, as revealed by selective inhibition. *Science* **277**, 1094–1097.

Bisogno T, Howell F, Williams G, Minassi A, Cascio MG, Ligresti A, Matias I, Schiano-Moriello A, Paul P, Williams EJ, Gangadharan U, Hobbs C, Di Marzo V & Doherty P (2003). Cloning of the first sn1-DAG lipases points to the spatial and temporal regulation of endocannabinoid signaling in the brain. *J Cell Biol* **163**, 463–468.

Bisogno T, MacCarrone M, De Petrocellis L, Jarrahian A, Finazzi-Agro A, Hillard C & Di Marzo V (2001). The uptake by cells of 2-arachidonoylglycerol, an endogenous agonist of cannabinoid receptors. *Eur J Biochem* **268**, 1982–1989.

Breivogel CS, Childers SR, Deadwyler SA, Hampson RE, Vogt LJ & Sim-Selley LJ (1999). Chronic delta9-tetrahydrocannabinol treatment produces a time-dependent loss of cannabinoid receptors and cannabinoid receptor-activated G proteins in rat brain. *J Neurochem* **73**, 2447–2459.

Cravatt BF, Demarest K, Patricelli MP, Bracey MH, Giang DK, Martin BR & Lichtman AH (2001). Supersensitivity to anandamide and enhanced endogenous cannabinoid signaling in mice lacking fatty acid amide hydrolase. *Proc Natl Acad Sci U S A* **98**, 9371–9376.

Devane WA, Hanus L, Breuer A, Pertwee RG, Stevenson LA, Griffin G, Gibson D, Mandelbaum A, Etinger A & Mechoulam R (1992). Isolation and structure of a brain constituent that binds to the cannabinoid receptor. *Science* **258**, 1946–1949.

Diana MA & Marty A (2004). Endocannabinoid-mediated short-term synaptic plasticity: depolarization-induced suppression of inhibition (DSI) and depolarization-induced suppression of excitation (DSE). *Br J Pharmacol* **142**, 9–19.

Franklin A & Stella N (2003). Arachidonylcyclopropylamide increases microglial cell migration through cannabinoid CB2 and abnormal-cannabidiol-sensitive receptors. *Eur J Pharmacol* **474**, 195–198.

Furshpan EJ, MacLeish PR, O'Lague PH & Potter DD (1976). Chemical transmission between rat sympathetic neurons and cardiac myocytes developing in microcultures: evidence for cholinergic, adrenergic, and dual-function neurons. *Proc Natl Acad Sci U S A* **73**, 4225–4229.

Gaoni Y & Mechoulam R (1964). Isolation, structure and partial synthesis of an active constituent of hashish. *J Am Chem Soc* **86**, 1646–1647.

Hajos N, Katona I, Naiem SS, MacKie K, Ledent C, Mody I & Freund TF (2000). Cannabinoids inhibit hippocampal GABAergic transmission and network oscillations. *Eur J Neurosci* **12**, 3239–3249.

Hajos N, Ledent C & Freund TF (2001). Novel cannabinoid-sensitive receptor mediates inhibition of glutamatergic synaptic transmission in the hippocampus. *Neuroscience* **106**, 1–4.

Hanus L, Abu-Lafi S, Fride E, Breuer A, Vogel Z, Shalev DE, Kustanovich I & Mechoulam R (2001). 2-Arachidonyl glyceryl ether, an endogenous agonist of the cannabinoid CB1 receptor. *Proc Natl Acad Sci U S A* **98**, 3662–3665.

Isokawa M & Alger BE (2005). Retrograde endocannabinoid regulation of GABAergic inhibition in the dentate gyrus granule cell. *J Physiol* **567**, 1001–1010.

Kathuria S, Gaetani S, Fegley D, Valino F, Duranti A, Tontini A, Mor M, Tarzia G, La Rana G, Calignano A, Giustino A, Tattoli M, Palmery M, Cuomo V & Piomelli D (2003). Modulation of anxiety through blockade of anandamide hydrolysis. *Nat Med* **9**, 76–81.

Katona I, Sperlagh B, Magloczky Z, Santha E, Kofalvi A, Czirjak S, Mackie K, Vizi ES & Freund TF (2000). GABAergic interneurons are the targets of cannabinoid actions in the human hippocampus. *Neuroscience* **100**, 797–804.

Kelley BG & Thayer SA (2004*a*). Anandamide transport inhibitor AM404 and structurally related compounds inhibit synaptic transmission between rat hippocampal neurons in culture independent of cannabinoid CB1 receptors. *Eur J Pharmacol* **496**, 33–39.

Kelley BG & Thayer SA (2004*b*). Delta9-tetrahydrocannabinol antagonizes endocannabinoid modulation of synaptic transmission between hippocampal neurons in culture. *Neuropharmacology* **46**, 709–715.

Kim J & Alger BE (2004). Inhibition of cyclooxygenase-2 potentiates retrograde endocannabinoid effects in hippocampus. *Nat Neurosci* **7**, 697–698.

Kreitzer AC, Carter AG & Regehr WG (2002). Inhibition of interneuron firing extends the spread of endocannabinoid signaling in the cerebellum. *Neuron* **34**, 787–796.

Kreitzer AC & Regehr WG (2001*a*). Cerebellar depolarization-induced suppression of inhibition is mediated by endogenous cannabinoids. *J Neurosci* **21**, RC174.

Kreitzer AC & Regehr WG (2001*b*). Retrograde inhibition of presynaptic calcium influx by endogenous cannabinoids at excitatory synapses onto Purkinje cells. *Neuron* **29**, 717–727.

Lenz RA, Wagner JJ & Alger BE (1998). N- and L-type calcium channel involvement in depolarization-induced suppression of inhibition in rat hippocampal CA1 cells. *J Physiol* **512**, 61–73.

Levison SW & McCarthy KD (1991). Characterization and partial purification of AIM: a plasma protein that induces rat cerebral type 2 astroglia from bipotential glial progenitors. *J Neurochem* **57**, 782–794.

Lichtman AH, Shelton CC, Advani T & Cravatt BF (2004). Mice lacking fatty acid amide hydrolase exhibit a cannabinoid receptor-mediated phenotypic hypoalgesia. *Pain* **109**, 319–327.

Llano I, Leresche N & Marty A (1991). Calcium entry increases the sensitivity of cerebellar Purkinje cells to applied GABA and decreases inhibitory synaptic currents. *Neuron* **6**, 565–574.

Lopez-Rodriguez ML, Viso A, Ortega-Gutierrez S, Fowler CJ, Tiger G, de Lago E, Fernandez-Ruiz J & Ramos JA (2003*a*). Design, synthesis and biological evaluation of new endocannabinoid transporter inhibitors. *Eur J Med Chem* **38**, 403–412.

Lopez-Rodriguez ML, Viso A, Ortega-Gutierrez S, Fowler CJ, Tiger G, de Lago E, Fernandez-Ruiz J & Ramos JA (2003*b*). Design, synthesis, and biological evaluation of new inhibitors of the endocannabinoid uptake: comparison with effects on fatty acid amidohydrolase. *J Med Chem* **46**, 1512–1522.

Lu B (2003). BDNF and activity-dependent synaptic modulation. *Learn Mem* **10**, 86–98.

Luk T, Jin W, Zvonok A, Lu D, Lin XZ, Chavkin C, Makriyannis A & Mackie K (2004). Identification of a potent and highly efficacious, yet slowly desensitizing CB1 cannabinoid receptor agonist. *Br J Pharmacol* **142**, 495–500.

Mackie K, Devane WA & Hille B (1993). Anandamide, an endogenous cannabinoid, inhibits calcium currents as a partial agonist in N18 neuroblastoma cells. *Mol Pharmacol* **44**, 498–503.

McLaughlin JP & Chavkin C (2001). Tyrosine phosphorylation of the mu-opioid receptor regulates agonist intrinsic efficacy. *Mol Pharmacol* **59**, 1360–1368.

Marcaggi P & Attwell D (2005). Endocannabinoid signaling depends on the spatial pattern of synapse activation. *Nat Neurosci* **8**, 776–781.

Marsicano G, Goodenough S, Monory K, Hermann H, Eder M, Cannich A, Azad SC, Cascio MG, Gutierrez SO, van der Stelt M, Lopez-Rodriguez ML, Casanova E, Schutz G, Zieglgansberger W, Di Marzo V, Behl C & Lutz B (2003). CB1 cannabinoid receptors and on-demand defense against excitotoxicity. *Science* **302**, 84–88.

Mato S, Chevaleyre V, Robbe D, Pazos A, Castillo PE & Manzoni OJ (2004). A single in-vivo exposure to delta 9THC blocks endocannabinoid-mediated synaptic plasticity. *Nat Neurosci* **7**, 585–586.

Matsuda LA, Lolait SJ, Brownstein MJ, Young AC & Bonner TI (1990). Structure of a cannabinoid receptor and functional expression of the cloned cDNA. *Nature* **346**, 561–564.

Melis M, Pistis M, Perra S, Muntoni AL, Pillolla G & Gessa GL (2004). Endocannabinoids mediate presynaptic inhibition of glutamatergic transmission in rat ventral tegmental area dopamine neurons through activation of CB1 receptors. *J Neurosci* **24**, 53–62.

Ohno-Shosaku T, Maejima T & Kano M (2001). Endogenous cannabinoids mediate retrograde signals from depolarized postsynaptic neurons to presynaptic terminals. *Neuron* **29**, 729–738.

Ohno-Shosaku T, Sawada S & Yamamoto C (1997). Properties of depolarization-induced suppression of inhibitory transmission in cultured rat hippocampal neurons. *Pfluger's Archiv* **435**, 273–279.

Ohno-Shosaku T, Tsubokawa H, Mizushima I, Yoneda N, Zimmer A & Kano M (2002). Presynaptic cannabinoid sensitivity is a major determinant of depolarization-induced retrograde suppression at hippocampal synapses. *J Neurosci* **22**, 3864–3872.

Oka S, Tsuchie A, Tokumura A, Muramatsu M, Suhara Y, Takayama H, Waku K & Sugiura T (2003). Ether-linked analogue of 2-arachidonoylglycerol (noladin ether) was not detected in the brains of various mammalian species. *J Neurochem* **85**, 1374–1381.

Pitler TA & Alger BE (1992). Postsynaptic spike firing reduces synaptic $GABA_A$ responses in hippocampal pyramidal cells. *J Neurosci* **12**, 4122–4132.

Reibaud M, Obinu MC, Ledent C, Parmentier M, Bohme GA & Imperato A (1999). Enhancement of memory in cannabinoid CB1 receptor knock-out mice. *Eur J Pharmacol* **379**, R1–R2.

Ronesi J, Gerdeman GL & Lovinger DM (2004). Disruption of endocannabinoid release and striatal long-term depression by postsynaptic blockade of endocannabinoid membrane transport. *J Neurosci* **24**, 1673–1679.

Ruano D, Lambolez B, Rossier J, Paternain AV & Lerma J (1995). Kainate receptor subunits expressed in single cultured hippocampal neurons: molecular and functional variants by RNA editing. *Neuron* **14**, 1009–1017.

Shen M & Thayer SA (1998). Cannabinoid receptor agonists protect cultured rat hippocampal neurons from excitotoxicity. *Mol Pharmacol* **54**, 459–462.

Sim LJ, Hampson RE, Deadwyler SA & Childers SR (1996). Effects of chronic treatment with delta9-tetrahydrocannabinol on cannabinoid-stimulated [35S]GTPgammaS autoradiography in rat brain. *J Neurosci* **16**, 8057–8066.

Stella N, Schweitzer P & Piomelli D (1997). A second endogenous cannabinoid that modulates long-term potentiation. *Nature* **388**, 773–778.

Sullivan JM (1999). Mechanisms of cannabinoid-receptor-mediated inhibition of synaptic transmission in cultured hippocampal pyramidal neurons. *J Neurophysiol* **82**, 1286–1294.

Thastrup O, Cullen PJ, Drobak BK, Hanley MR & Dawson AP (1990). Thapsigargin, a tumor promoter, discharges intracellular Ca^{2+} stores by specific inhibition of the endoplasmic reticulum Ca^{2+}-ATPase. *Proc Natl Acad Sci U S A* **87**, 2466–2470.

Topham MK & Prescott SM (2002). Diacylglycerol kinases: regulation and signaling roles. *Thromb Haemost* **88**, 912–918.

Trettel J, Fortin DA & Levine ES (2004). Endocannabinoid signalling selectively targets perisomatic inhibitory inputs to pyramidal neurones in juvenile mouse neocortex. *J Physiol* **556**, 95–107.

Vincent P, Armstrong CM & Marty A (1992). Inhibitory synaptic currents in rat cerebellar Purkinje cells: modulation by postsynaptic depolarization. *J Physiol* **456**, 453–471.

Walter L & Stella N (2003). Endothelin-1 increases 2-arachidonoyl glycerol (2-AG) production in astrocytes. *Glia* **44**, 85–90.

Wilson RI & Nicoll RA (2001). Endogenous cannabinoids mediate retrograde signalling at hippocampal synapses. *Nature* **410**, 588–592.

Witting A, Walter L, Wacker J, Moller T & Stella N (2004). P2X7 receptors control 2-arachidonoylglycerol production by microglial cells. *Proc Natl Acad Sci U S A* **101**, 3214–3219.

Acknowledgements

This work was supported by grants from the National Institute on Drug Abuse DA11322, DA00286 and DA13410 (K.M.) and DA15916 (to Charles Chavkin). We would like to thank J. Sullivan and N. Stella for critical readings of the manuscript.